15th International Symposium on Flow Visualization
June 25-28, 2012, Minsk, Belarus

VISUALIZATION OF FLOW FIELDS ABOUT AN AIRFOIL WITH A GURNEY FLAP

Y. TAKAKURA[1c], T. KOBAYASHI[2], M. TAKAGI[3]

[1]Department of Prime Mover Engineering, Tokai University, Hiratsuka, Kanagawa 259-1292, Japan
[2]School of Engineering, Graduate School of Tokai University, Hiratsuka, Kanagawa 259-1292, Japan
[3]Takagi Engineering, Kamakura, Kanagawa, 247-0064, Japan

[c]Corresponding author: Tel.: +81-463-58-1211; Fax: +81-463-59-8293; Email: takakura@tokai-u.jp

KEYWORDS:

Main subjects: Gurney flap, aerodynamic characteristics, flow visualization
Fluid: incompressible flows
Visualization method(s): tuft method, smoke method
Other keywords: coefficients of lift, coefficients of drag, polar curves

ABSTRACT: The Gurney flap is a high-lift device with a L shape beam attached at the trailing edge of the lower surface of a wing. The aim of this paper is to show effects of the Gurney flaps for aerodynamic characteristics of NACA4412 airfoil and visualization of the flow fields in wind-tunnel experiments. The height of flaps is 0 to 6% of the chord length, Reynolds number was 6.5×10^5, and measurement condition is three-dimensional (3D) or quasi two-dimensional (2D), according to flow fields without or with side plates. The Gurney flaps made C_L and stall angles higher: in 3D cases, the stall angles remarkably increased as the mounted flap was higher, while in 2D cases C_L increased far more than in 3D cases at same attack angles. Flow visualization confirmed the reason: near the symmetric plane at the wing center the flow direction is changed more by higher flaps, and the reaction force acts as the lift; the growth of wingtip vortex by higher flaps causes the increase of stall angles in 3D cases while quasi two-dimensionality is maintained in 2D cases. Further it has been found that each family of polar curves for 2D or 3D measurements constitutes a curve like an envelope. By use of the “envelope”, when the necessary value of C_L is given, the combination of an attack angle and a flap height with the lowest value of C_D can be obtained. As concluding remarks, usage of Gurney flaps is effective to obtain high C_L with small and light wings, or when C_D increases within tolerance level.

INTRODUCTION. In the case of road vehicles, shape optimization and equipment of aerodynamic devices such as wings enhances the downforce, i.e., negative lift, and consequently does the friction force of tires against the road. This effect brings race cars the running stability, so that they can turn curves with high speed without sideslips. The downforce can be furthermore increased by adding high-lift devices to wings, as the lift force in the case of airplanes.

The Gurney flap, named after the deviser Dan Gurney, is a high-lift device with a L-shape beam, attached at the trailing edge on the lower surface of a wing. It has been used for high-speed road vehicles since 1970s. As regulations of car races restrict sizes of a vehicle including wing areas, the Gurney flaps are frequently equipped in race cars of Formula One, etc., because of their compactness and lightness, to obtain the high-speed running stability at curves.

Effects of the Gurney flaps have been investigated by Liebeck[1], Kats[2], Jang[3] and Storms[4], for the limited range of flap heights less than 3% of the chord length in two-dimensional flow fields, probably because the maximum lift-drag ratio was obtained with the flap height of 0.5% chord length in their reports. In wings of actual race cars, however, the lift itself or the lift-weight ratio is more important than the lift-drag ratio, and the flap height is supposed more than 3% chord length. Moreover, wings are mounted with side plates (quasi two-dimensional case), with winglets, or without them (three-dimensional case).

In this study, effects of the Gurney flaps are investigated for NACA4412 airfoil, not only in quasi two-dimensional cases but also in three-dimensional cases. The range of flap heights is extended to 6% of the chord length. For the change of flap heights and attack angles the aerodynamic characteristics are measured in wind-tunnel experiments, and discussion is further verified by flow visualization.

EXPERIMENTAL SETUP.

EXPERIMENTAL INSTRUMENTATIONS. In experiments the large-scale low-speed wind tunnel of Tokai University has been used. The wind tunnel is single-return closed-circuit type with an open jet test section, the dimension of which is 1m high and 1.5m wide at the nozzle exit, and 2m long. Aerodynamic characteristics are measured by a strut-type six component balance, and data in electric signals are taken into a personal computer through an A/D converter.

EXPERIMENTAL MODEL. The NACA4412 airfoil is adopted as a basic shape, because of desirable stall properties for wide range of Reynolds number. The wing dimension is given by 500mm in chord length and 900mm in width (aspect ratio: 1.8). As Gurney flaps L-shape angle irons in width of 900mm are adopted. The flap heights are 0% chord (without flap), 1% chord (5mm), 2% chord (10mm), 3% chord (15mm), 4% chord (20mm), 5% chord (25mm), and 6% chord (30mm), and the angle irons are attached to the trailing edge on the lower surface of the wing (Fig.1). The model of the wing is, with upper side down, supported by the main strut (at 50mm from the leading edge) and the sub strut (at 100mm from the trailing edge) in order to reduce interferences of flows near the flap with the struts (Fig.2).

MEASUREMENT CONDITIONS. Wind velocity is set to 19.5 m/s ($Re=6.5\times10^5$), and angles of attack are changed in ranges that the stall angle is detected for each case with a flap height. As flow-field conditions two cases are prepared: one is the three-dimensional (3D in short) flow field where a wing model is set alone, and the other is the quasi two-dimensional (2D in short) flow field, where a wing model is set with acrylic side plates of 1100mm×1380mm, as shown in Fig.3. There is 5mm gap between a wingtip and a side plate at either end to change the attack angle.

Lift force L, drag force D and pitching moment M_P are measured with sampling of 1024 data at 10ms intervals. Measurements are repeated three times for each case with a flap height in 2D or 3D flows for attack angle α, and their average is used as a measurement value. Aerodynamic characteristics are discussed[5,6] by the following quantities[7]: coefficient of lift C_L, coefficient of drag C_D, coefficient of pitching moment C_M around the experimental moment center (position supported by the main strut) x_{MC}, coefficient of pitching moment C_{MAC} around the aerodynamic center $x_{C/4}$, lift-drag ratio L/D, and position of the center of pressure x_{CP}.

VISUALIZATION TECHNIQUE. Flows are visualized by the smoke method and the surface-tuft method. Smoke visualizes flows near the wing center and wingtip. Surface tufts visualize flows on the lower surface of the wing. Tufts are attached to grid points of 50mm intervals for range of 25mm to 475 mm upstream from the trailing edge and 25mm intervals for range of 10mm to 475mm inside from the wingtip.

Fig.1 Model of wing equipped with Gurney flap

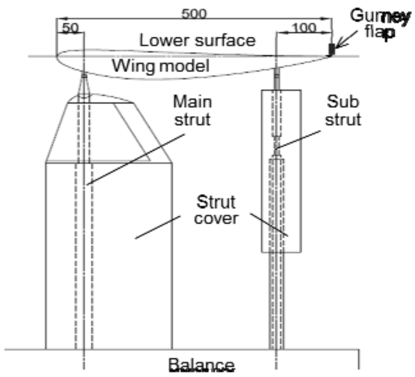

Fig.2 Wing model supported by main and sub struts

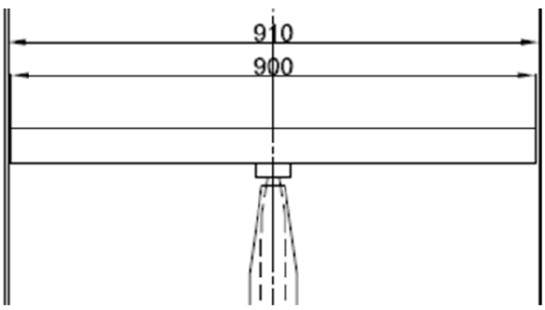

Front view

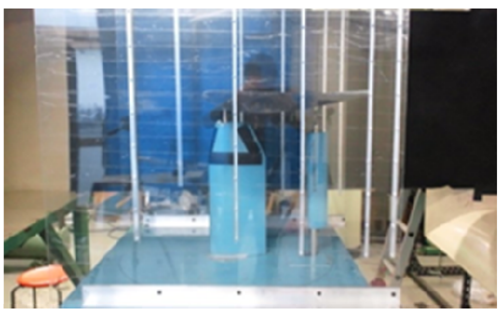

Side view

Fig.3 Quasi two-dimensional flow field with side plates

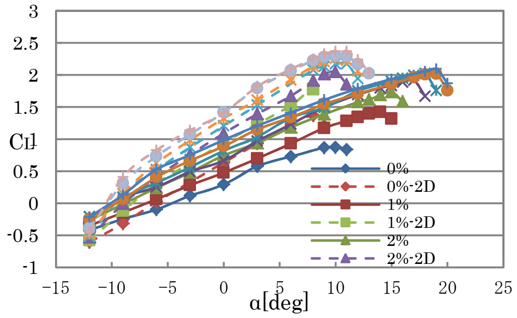

(a) C_L-α curves

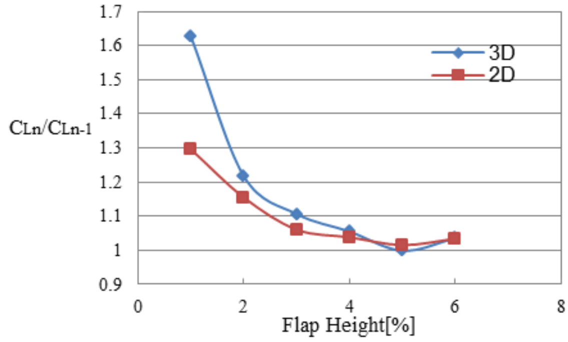

(e) Increasing ratio of maximum C_L

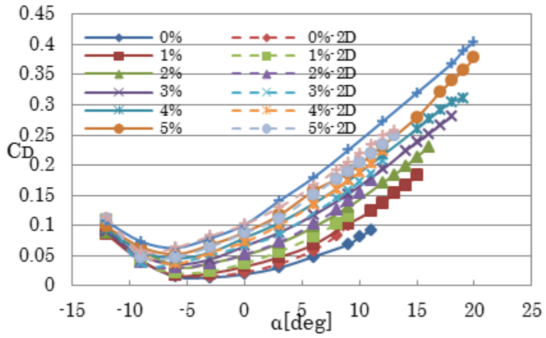

(b) C_D-α curves

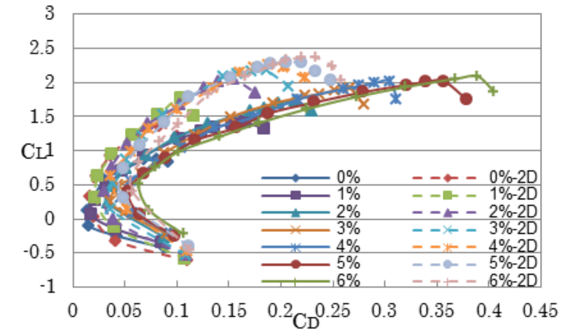

(f) Polar curves

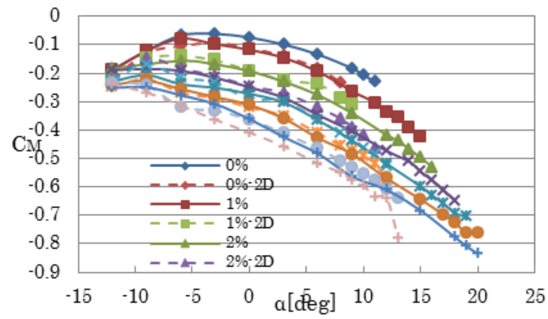

(c) C_M-α curves

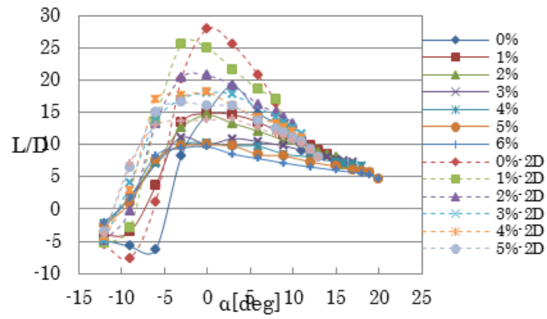

(g) L/D-α curves

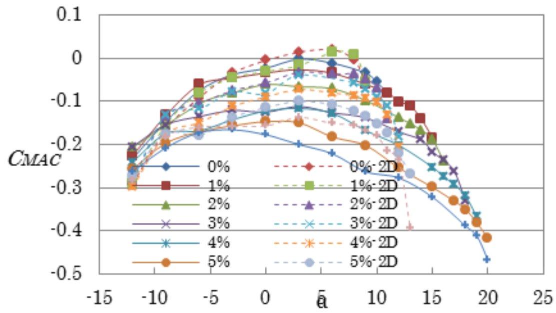

(d) C_{MAC}-α curves

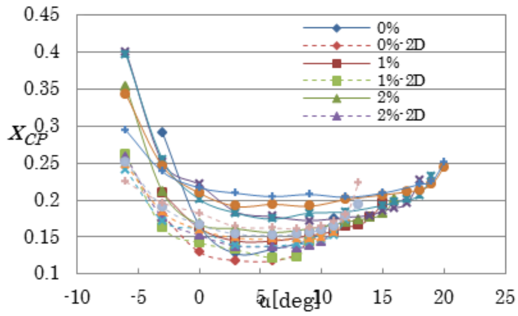

(h) x_{CP}-α curves

Fig.4 Aerodynamic characteristics

RESULTS AND DISCUSSION.

AERODYNAMIC CHARACTERISTICS. Figure 4 shows effects of Gurney flaps for aerodynamic characteristics of the NACA4412 airfoil, where solid lines indicate 3D cases and broken lines do 2D cases.

In C_L-α curves shown in Fig.4 (a), maximum values of C_L and stall angles increase as the flaps become higher both in 3D and 2D flow fields. Comparing curves of each family, the following tendencies are observed:
i) C_L values are higher in 2D cases than in 3D cases for a same flap height in a same attack angle; and
ii) stall angles are higher in 3D cases than in 2D cases for a same flap hight.
It is considered that the above tendencies would be caused by existence or nonexistence of wingtip vortices. In 3D cases, near the wingtip the fluids whirl from the lower wing surface with higher pressure to the upper wing surface with lower pressure, so that the pressure difference might be reduced. Therefore in 3D cases C_L is less than in 2D cases. Regarding the stall angles, the reason why in 3D cases they increase more than in 2D cases as the flaps become higher would be that flow reattachments caused by wingtip vortices prevent the flow separation on the upper wing surface.

In C_D-α curves of Fig.4 (b), C_D increases even at a same attack angle as the mounted flaps become higher both in 3D and 2D flow fields. In C_M-α curves of Fig.4 (c), C_M increases towards negative direction in 2D cases more than in 3D cases. This can also be explained by existence or nonexistence of wingtip vortices, because in 2D cases the side plates suppress generation of wingtip vortices and therefore the pressure would increase near the trailing edge on the lower wing surface. C_M is transformed into C_{MAC}, and C_{MAC}-α curves are shown in Fig.4 (d). It is confirmed that C_{MAC}-α curves become mostly flat in a suitable range of attack angles.

Figure 4 (e) shows the increasing ratios of maximum C_L when the flap height becomes large by 1% of the chord length. In both 2D and 3D cases for the flaps lower than 3% chord the increasing ratios are over 1.1, while for the flaps higher than 3% chord they are mostly constant with values under 1.1.

Regarding Fig.4 (f), each family of polar curves for 2D or 3D measurements constitutes a curve like an envelope. In Fig.5 measured points on two "envelopes" are plotted, where a symbol with a small letter is for 3D cases and a symbol with a capital letter is for 2D cases. By use of each "envelope", when the necessary value of C_L is given, combination of an attack angle and a flap height with the lowest value of C_D can be obtained.

In *L/D*-α curves of Fig.4 (g) maximum *L/D* decreases as the flap becomes higher; it decreases about 50% from 0% to 6% chord in both 2D and 3D cases. The maximum *L/D* is higher in 2D cases than in 3D cases, probably because the side plates prevent generation of the wingtip vortices and increase C_L in 2D cases, as shown in C_L-α curves of Fig.4 (a).

Figure 4 (h) indicates that the position of the center of pressure closest to the leading edge for changes of attack angle moves downstream as the flap becomes higher.

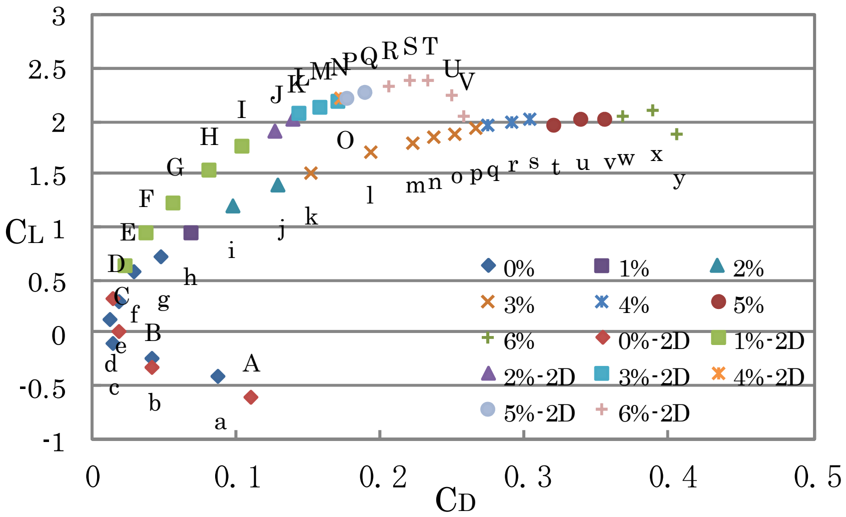

Fig.5 Points on 2D and 3D envelopes

3D (without side plates) 2D (with side plates)

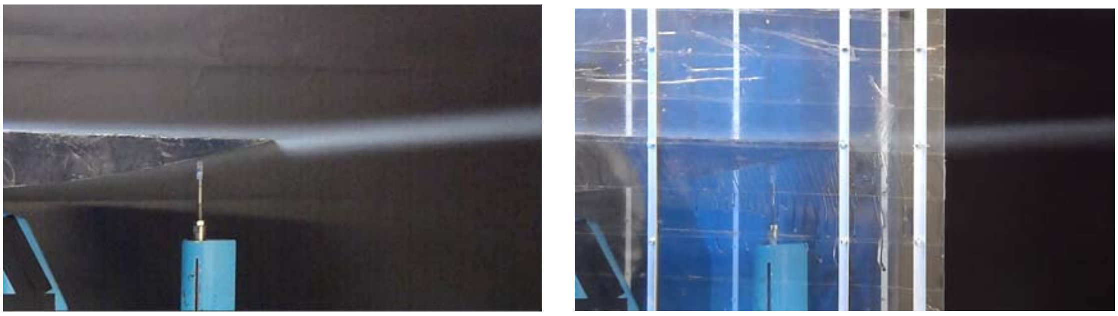

(a) 0% chord flap (without flap)

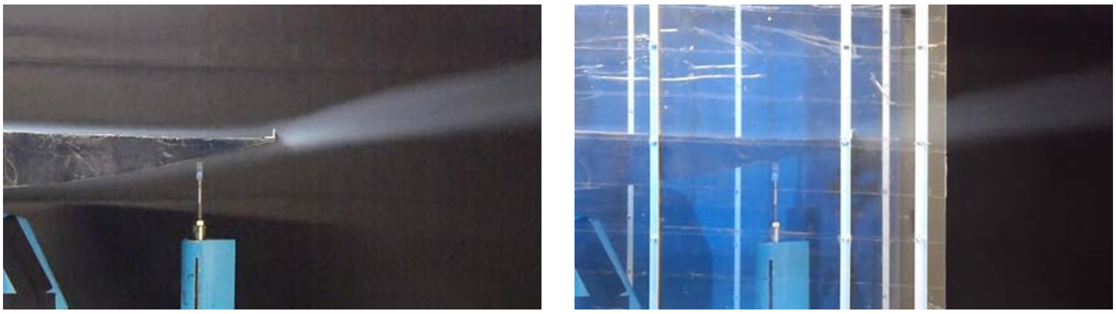

(b) 2% chord flap

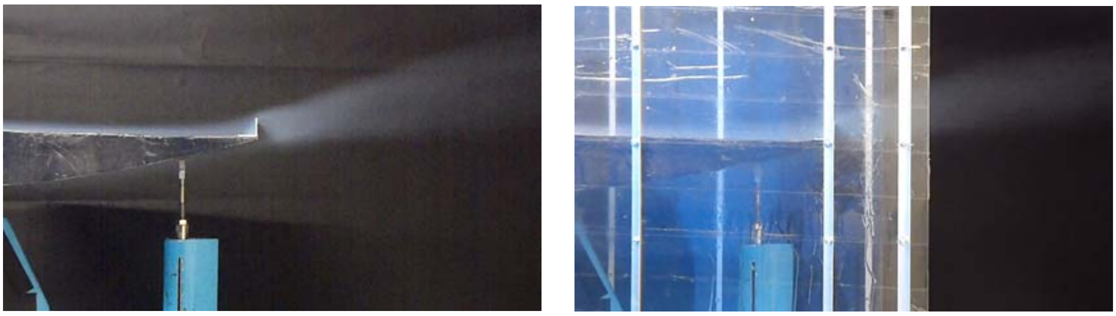

(c) 4% chord flap

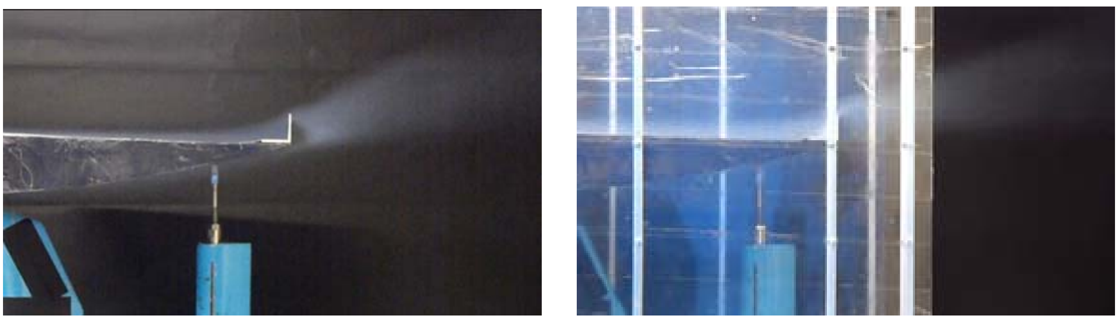

(d) 6% chord flap

Fig.6 Smoke visualization near symmetric plane at wing center; left and right pictures are for 3D flow fields and 2D ones, respectively

3D (without side plates) 2D (with side plates)

(a) 0% chord flap (without flap)

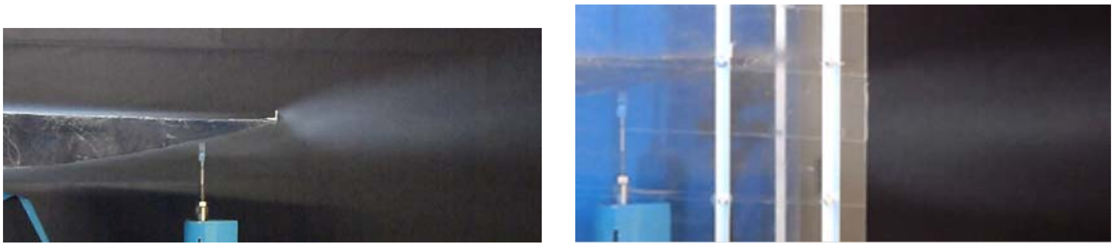

(b) 2% chord flap

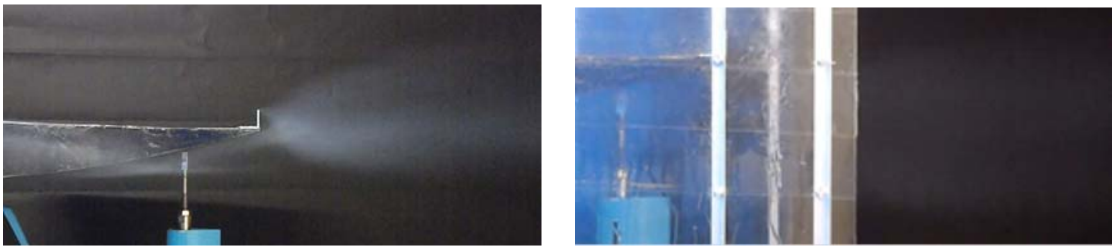

(c) 4% chord flap

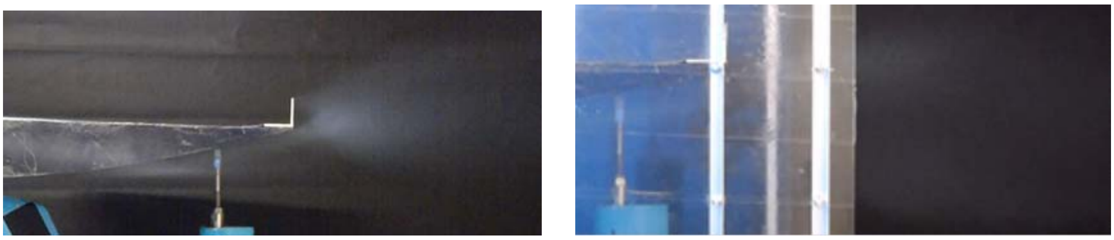

(d) 6% chord flap

Fig.7 Smoke visualization at wingtip; left and right pictures are for 3D flow fields and 2D ones, respectively

3D (without side plates) 2D (with side plates)

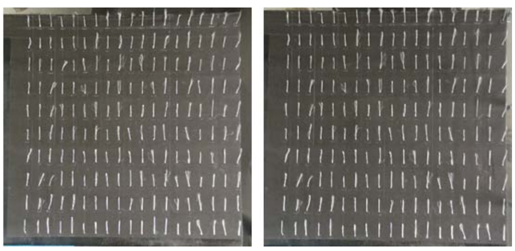

(a) 0% chord flap (without flap)

3D (without side plates) 2D (with side plates)

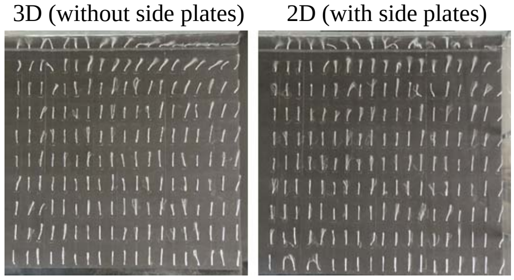

(b) 6% chord flap

Fig.8 Flow visualization on lower wing surface by tufts

FLOW VISUALIZATION. Experiments have been carried out for visualization of flows about the models with flap heights of 0%, 2%, 4%, and 6% chord length, and cases of attack angle zero are shown here.

Figure 6 shows visualization of flows near the symmetric plane at the wing center by the smoke method, where left and right pictures are all for 3D flow fields and 2D ones with side plates, respectively. In Fig.6 (a) without flaps the smoke directions are slightly changed in both pictures. In each flow field the higher the Gurney flap is, the more the smoke direction is changed toward the lower wing-surface side (upside of the picture) near the flap, as clearly shown in the case of 6% chord flap in Fig.6 (d). Therefore it is confirmed that higher flaps have higher lift forces by the reaction force from the flowing fluid to the wing. Although near the wing center flows are similar between 3D and 2D cases, wingtip flows shows discrepancy between them, as shown in smoke flows of Figs.7 (a) to (d). In the 3D flow fields (left pictures) wingtip vortex is observed, and the vortex grows larger as a higher flap is mounted. On the other hand, in the 2D flow fields (right pictures), instead of the wingtip vortex, smoke diffuses in downstream of the trailing edge largely toward the upper wing-surface side (downside of the picture), and it diffuses also toward the lower wing-surface side (upside of the picture) as flaps become higher. The visualization supports the discussion about Fig.4 (a) in the previous section that in 3D cases reattachment of wingtip vortex makes stall angles higher for increase of the flap height, and that in 2D cases generation mechanism of the lift force by the reaction force from the airflow to the wing holds even at wingtip to make C_L higher than in 3D cases.

Figure 8 shows visualization of flows on the lower wing surface by tufts, where the top and right ends of the pictures correspond to the trailing edge and the wingtip, respectively. Comparing left pictures in Figs.8 (a) and (b), in 3D cases influences of the wingtip vortex in the right end line are observed at an almost same location whether the flap is mounted or not. The difference appears near the trailing edge: the area of tufts which point to the wingtip direction is larger in the case with the 6% chord flap probably because of growth of the wingtip vortex. In 2D cases shown in right pictures of Figs.8 (a) and (b), tufts only on the right end line point to the gap between the wingtip and the end plate both in the cases with and without the flap. Further in the case with the 6% chord flap, tufts only on the top row near the trailing edge fall into disorder. Therefore surface-tuft visualization also indicates that the growth of wingtip vortex by the flap causes the increase of stall angles in 3D cases while quasi two-dimensionality is maintained in 2D cases.

CONCLUDING REMARKS. Effects of Gurney flaps were investigated for aerodynamic characteristics of NACA4412 airfoil by wind-tunnel experiments, and with supports of flow visualization, the following conclusions were obtained.

1) The Gurney flaps make C_L and stall angles higher: in 3D cases the stall angle remarkably increases as the mounted flap is higher, while in 2D cases, C_L increases far more than in 3D cases at the same attack angle.
2).Each family of polar curves for 2D or 3D flow fields constitutes a curve like an envelope. By use of each “envelope”, when the necessary value of C_L is given, combination of an attack angle and a flap height with the lowest value of C_D can be obtained.
3) Flow visualization confirmed the causes of 1): near the symmetric plane at the wing center the flow direction is changed more by higher flaps, and the reaction force acts as the lift force; the growth of wingtip vortex by higher flaps causes the increase of stall angles in 3D cases while quasi two-dimensionality is maintained in 2D cases.

Finally, The Gurney flaps have advantages of effective lift-weight ratio and compactness. Usage of Gurney flaps would be hopeful to obtain high C_L with small and light wings, or when C_D increases within tolerance level under extra engine power.

References

1. Liebeck, R. H. *Design of Subsonic Airfoils for High Lift*. Journal of Aircraft, Vol.15, No.9, 1978, p.547-561
2. Katz, J. and Dykstra, L. *Study of an Open-Wheel Racing-Car’s Rear-Wing Aerodynamics*. Society of Automotive Engineers, technical paper series 890600, 1989
3. Jang, C. S., Ross, J. C., and Cummings, R. M. *Computational Evaluation of an Airfoil with a Gurney Flap*. A collection of technical papers, 10th AIAA Applied Aerodynamics Conference, AIAA-92-2708-CP, 1992

4. Storms, B. L. and Jang, C. S. *Lift Enhancement of an Airfoil Using a Gurney Flap and Vortex Generators*. Journal of Aircraft, Vol.31, No.3, 1994, p.542-547
5. Kobayashi, T., Takakura, Y., and Takagi, M. *Effects of Gurney Flaps for Aerodynamic Characteristics of an Airfoil*. Theoretical and Applied Mechanics Vol.61 (submitted).
6. Kobayashi, T., Takakura, Y., and Takagi, M. *Effects of Gurney Flaps for Aerodynamic Characteristics of an Airfoil (2)*. JSASS (Japan Society of Aeronautical and Space Sciences) 44th Fluid Dynamics Conference, 2012 (in Japanese).
7. Kermode, A. C. *Mechanics of Flight*, 10th edition, Revised and edited by Barnard, R. H. and Philpott, D. R., Longman, 1996, p.70-125